Mass Spectrometry

DOI: 10.1002/ange.201004861

Detecting Reaction Intermediates in Liquids on the Millisecond Time Scale Using Desorption Electrospray Ionization**

*Richard H. Perry, Maurizio Splendore, Allis Chien, Nick K. Davis, and Richard N. Zare**

The ability to detect reactive intermediates in solution using mass spectrometry (MS) has significantly advanced in the last decade owing to the development of atmospheric pressure ionization methods such as electrospray ionization (ESI).[1,2] The recent invention of desorption electrospray ionization (DESI)[3] allows samples to be directly ionized in the open environment and introduced into the mass spectrometer without the need for sample pretreatment. These features make DESI easily amenable to high-throughput analyses and increase the variety of samples that can be analyzed by MS.[4,5,6] In DESI, charged droplets in a stream of gas are directed at an analyte of interest, which has been deposited on a surface. Upon impact, analyte molecules are extracted from the surface into secondary microdroplets, from which gas-phase ions are eventually formed.[5,7] By adding reagents to the spray, it is possible to perform reactions with compounds adsorbed on surfaces and monitor the products in real time.[8] Transfer hydrogenation using Ru organometallic catalysts in the presence of a hydrogen donor is a simple, efficient, nonhazardous, and highly enantioselective approach for the reduction of multiple bonds.[9,10,11] The asymmetric reduction of carbonyl bonds to form chiral alcohols is an important reaction in nature and in organic syntheses.[9,12] One approach to synthesizing Ru^{II} asymmetric transfer hydrogenation catalysts is to react $[\{RuCl_2(p\text{-cymene})\}_2]$ (**1**) with amino alcohol ligands (**L**) such as (1***R***, 2***S***)-*cis*-1-amino-2-indanol (**2**; Scheme 1a).[2,13,14] Our research group has studied these organometallic reactions at room temperature and atmospheric pressure by placing **1** on a surface and **L** in the nebulizer spray of a DESI source. Herein, we demonstrate for the first time that DESI can intercept reactive intermediates formed in the secondary microdroplets on the millisecond timescale.

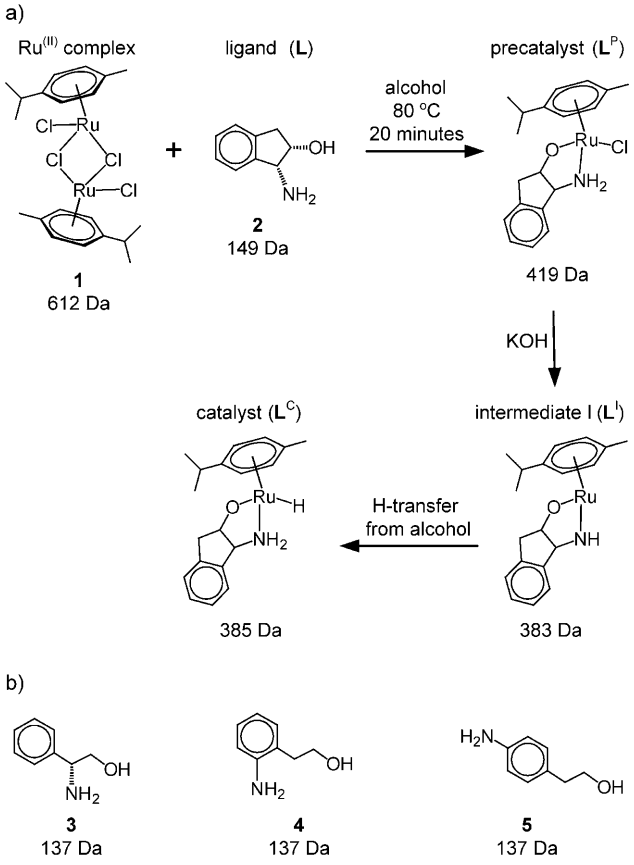

Scheme 1. a) Proposed mechanism for the formation of a Ru^{II} asymmetric hydrogen-transfer catalyst from the reaction of $[\{RuCl_2(p\text{-cymene})\}_2]$ (**1**) with (1***R***, 2***S***)-*cis*-1-amino-2-indanol (**2**). The stated experimental conditions refer to reactions carried out with bulk quantities.[2,14] b) The structures of other ligands studied: (***R***)-2-phenylglycinol (**3**), 2-aminophenethyl alcohol (**4**), and 4-aminophenethyl alcohol (**5**).

The analysis of **1** (5 μL of 5×10^{-3} M solution in CH_2Cl_2 deposited on paper) by DESI using CH_3OH as the reagent spray solution (liquid flow rate = 10 μL min^{-1}; N_2 flow rate = 0.6 L min^{-1}; spray voltage = 5 kV) resulted in signals corresponding to the isotopic distributions at *m/z* 559, *m/z* 579, and *m/z* 634, which are produced by fragmentation and reaction of **1** with CH_3OH and H_2O (Figure 1a; the assignment of these signals will be discussed later). From this point forward specific isotopic distributions will be referred to using the *m/z* ratio of the most abundant signal. When amino alcohol **2** (10^{-4} M solution in CH_3OH) was introduced as a

[*] Dr. R. H. Perry, N. K. Davis, Prof. R. N. Zare
Department of Chemistry, Stanford University
333 Campus Drive, Stanford, CA 94305-5080 (USA)
Fax: (+650) 725-0259
E-mail: zare@stanford.edu
Dr. M. Splendore, Dr. A. Chien
Stanford University Mass Spectrometry
Stanford University
333 Campus Drive, Stanford, CA 94305-5080 (USA)

[**] We are indebted to Prof. Robert Waymouth (Stanford University) for insightful comments and help in determining reasonable chemical structures, Dr. Antonio De Crisci (Stanford University) for suggesting the ruthenium hydrogen-transfer catalyst, and Prof. R. Graham Cooks (Purdue University) for encouraging the study of desorption electrospray ionization reactions. Financial support from the Air Force Office of Scientific Research (FA 9550-10-1-0235) is gratefully acknowledged.

Supporting information for this article is available on the WWW under http://dx.doi.org/10.1002/anie.201004861.

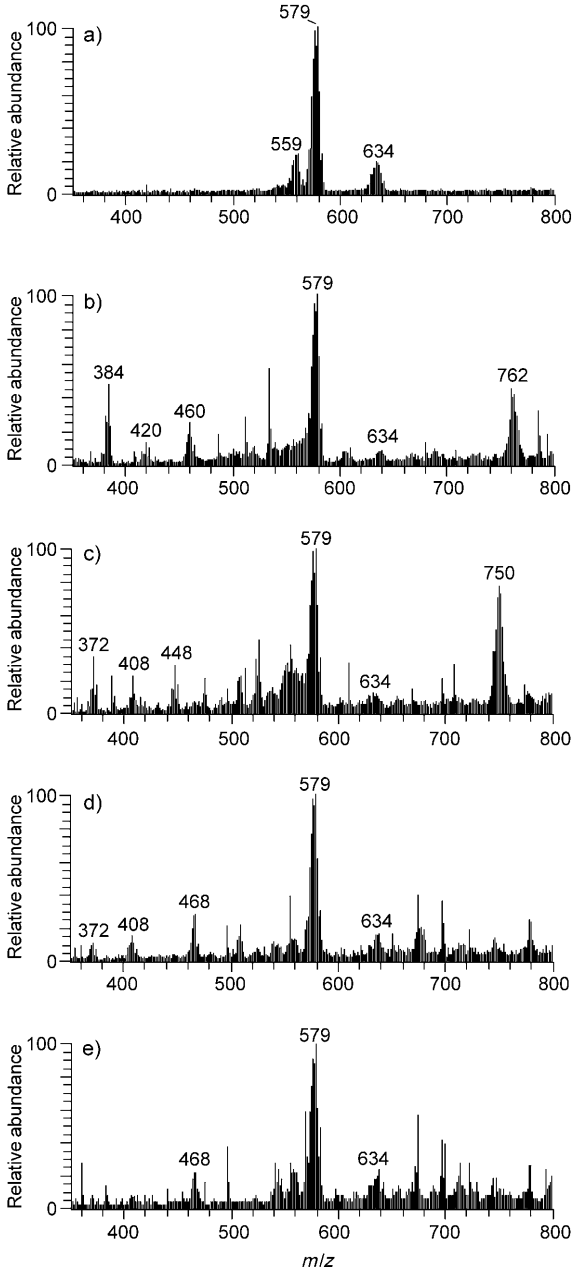

Figure 1. DESI mass spectra of **1** deposited on paper using in the spray a) CH_3OH, b) **2**, c) **3**, d) **4**, and e) **5**. The concentration of the ligands **2**–**5** is 10^{-4} M in CH_3OH. Assignments of major signals are described in the text.

reagent in the nebulizer spray (Figure 1b), additional isotopic distributions are observed at *m/z* 420 and *m/z* 384, which correspond to the protonated forms of the precatalyst ($\mathbf{L^P}$), and a mixture of intermediate I ($\mathbf{L^I}$) and the catalyst ($\mathbf{L^C}$). From this point forward, specific reactive species will be designated by substituting "**L**" with the numerical label for **L** (Scheme 1). For example, intermediate I formed by reacting **4** with **1** is designated $\mathbf{4^I}$. The observation of these species in the mass spectra of the reaction of **2** with **1** agrees with previous offline analyses of the bulk reaction carried out by ESI-MS.[2] Furthermore, the proposed structures of $\mathbf{L^P}$, $\mathbf{L^I}$, and $\mathbf{L^C}$ are supported by previously published X-ray crystallographic structures of the analogous reactive species formed in the reaction of **1** with 1,2-diamines.[11]

One of the most exciting features of the mass spectrum shown in Figure 1b is the signal at *m/z* 762, which corresponds to the protonated form of the coordination species of **2** with **1**. A similar distribution is observed at *m/z* 750 when **3** was used as the reagent (Figure 1c and see Scheme 1b for structure), as well as the corresponding $\mathbf{L^P}$ and $[\mathbf{L^I}+\mathbf{L^C}]$ distributions at *m/z* 408 ($\mathbf{3^P}$) and *m/z* 372 ($[\mathbf{3^I}+\mathbf{3^C}]$). From this point forward, the coordination species of **L** with **1** will be designated intermediate II ($\mathbf{L^{II}}$). Note that the species produced from **3** have masses that are 12 Da less than the corresponding species produced in the reaction of **2** with **1**. Interestingly, when the amine group is located on a carbon atom that is farther away from the OH functionality (**4** and **5**; see Scheme 1b for structures), the coordination complex at *m/z* 750 is not observed (Figure 2d,e). Because the formation of these ionic species depends on the relative positions of the NH_2 and OH groups on the ligand **L**, this behavior strongly indicates that *m/z* 762 ($\mathbf{2^{II}}$) and *m/z* 750 ($\mathbf{3^{II}}$) represent intermediates in the reaction of **1** with **2** or with **3**. Similarly, another reaction intermediate is detected at *m/z* 460 and *m/z* 448 (*m/z* difference of 12 Da) for the reaction of **1** with **2** or with **3** (designated intermediate III ($\mathbf{L^{III}}$); *m/z* 460 and *m/z* 448 correspond to $\mathbf{2^{III}}$ and $\mathbf{3^{III}}$, respectively), however, this intermediate is not detected for the ligands that have a greater distance between the NH_2 and OH groups. These results indicate that formation of $\mathbf{L^{II}}$ and $\mathbf{L^{III}}$ of **4** and **5** is not as thermodynamically or kinetically favored as the reactive intermediates formed from the β-amino alcohols.

The signals at *m/z* 408 and *m/z* 372 in Figure 1d indicate that **4** also reacts with **1** to produce $\mathbf{4^P}$ and $[\mathbf{4^I}+\mathbf{4^C}]$. A comparison of the sum of the signal areas[15] for *m/z* 372 and *m/z* 408 for **3** ($120\pm6\times10^7$) and **4** ($16\pm2\times10^7$) suggests that in the same time period, **3** produces 7.6 ± 1.0 times more of these species than **4** under the same experimental conditions (unless specified otherwise, areas and intensities are obtained by integrating signals for the first 15 seconds of the analysis, errors represent one standard deviation calculated from three measurements, and ten spectra are averaged per measurement). A similar comparison for **2** ($114\pm1\times10^7$) and **3** illustrates that they produce similar amounts of $\mathbf{L^P}$ and $[\mathbf{L^I}+\mathbf{L^C}]$, which is not surprising owing to the similarity of their chemical structures and previous reports[14] demonstrating that the rate of the bulk catalytic reaction is similar for **2** and **3**. For example, when acetophenone is the substrate, 1-phenylethanol is produced with yields of 70% in 1.5 hours and 95% in 2 hours for **2** and **3** (i.e. a ratio of ca. 1.2).[14] Furthermore, the intensity of $\mathbf{L^P}$ and $[\mathbf{L^I}+\mathbf{L^C}]$ relative to *m/z* 579 is generally lower for **4** ($5\pm3\%$ and $9\pm2\%$) compared with **2** ($6\pm2\%$ and $17\pm5\%$) and **3** ($9\pm1\%$ and $13\pm2\%$). These lower abundances demonstrate that the reaction is more favored when the NH_2 and OH groups of **L** are located on adjacent carbon atoms, thus providing additional support for the assignment of the $\mathbf{L^{II}}$ and $\mathbf{L^{III}}$ intermediates in the reaction of **1** with β-amino alcohols.

When solutions of **1** and **L** are infused into a static mixing tee followed by online ESI-MS,[16] $\mathbf{L^{II}}$ and $\mathbf{L^{III}}$ are not observed in the acquired mass spectra (data not shown) because the

reaction time is longer (ca. 15 s) compared with the reaction time in the desorbed microdroplets of DESI (a few milliseconds for a droplet velocity of ca. 4 $m\,s^{-1}$[17] and a separation distance of ca. 0.5 cm between the spot and the inlet of the mass spectrometer). These results are in agreement with previous offline ESI-MS analyses of the bulk reaction, in which only the $\mathbf{L}^{\mathbf{P}}$, $\mathbf{L}^{\mathbf{I}}$, and $\mathbf{L}^{\mathbf{C}}$ were reported.[2] For **2** and **3**, $[\mathbf{L}^{\mathbf{I}}+\mathbf{L}^{\mathbf{C}}]$ is the most abundant distribution in ESI mass spectra (absolute abundance is ca. 2×10^7 for both ligands) and all the other signals have relative intensities lower than approximately 15%. However, for **4** and **5**, species formed from the reaction of **1** with CH_3OH are the most abundant and have absolute intensities similar to experiments in which **1** and CH_3OH were infused into the mixing tee (absolute abundance is ca. 2×10^8 for all cases).[18] All other signals in ESI mass spectra of the reaction of **1** with **4** or **5** have relative intensities lower than approximately 15%. Furthermore, the relative intensity of $[\mathbf{4}^{\mathbf{I}}+\mathbf{4}^{\mathbf{C}}]$ is approximately 2% and no reactive species were observed for **5**. These results demonstrate that **2** and **3** react faster with **1** compared with **4** and **5**. All the ESI results are consistent with those obtained using DESI (Figure 1), thereby providing additional support for the claims that the NH_2 and OH positions play an important role in the formation of $\mathbf{L}^{\mathbf{II}}$ and $\mathbf{L}^{\mathbf{III}}$ and that these intermediates are relevant to the reaction mechanism.

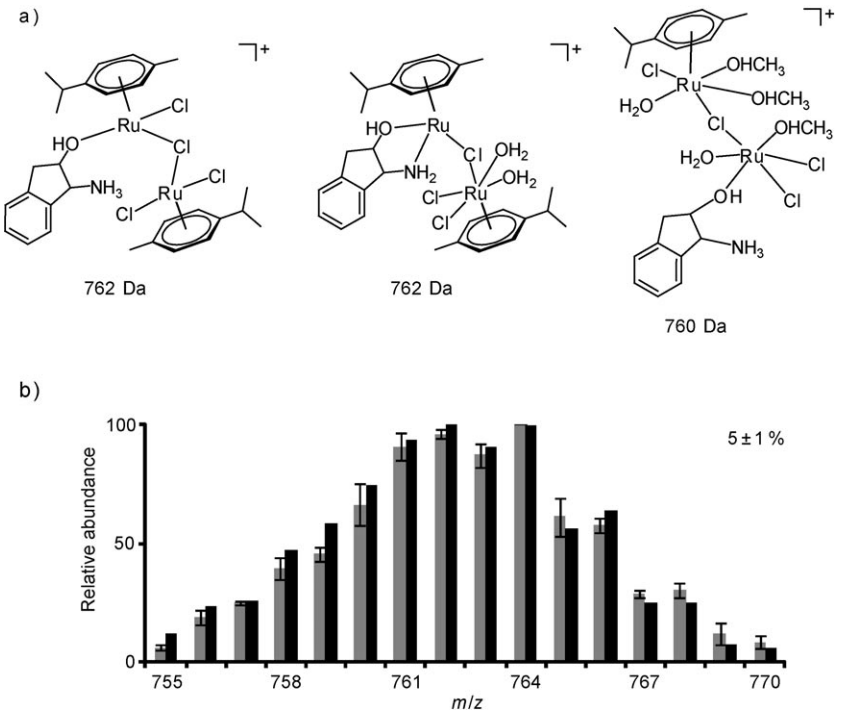

Figure 2. a) Possible structures for some of the reactive species at *m/z* 762 formed in the reaction of **1** with **2**. b) Comparison of the experimental (gray) and calculated (black) isotopic distributions of intermediate II ($\mathbf{L}^{\mathbf{II}}$) formed from the reaction of **1** (15 μg deposited on paper) with **2**. The concentration of **2** is 10^{-4} M in CH_3OH. The distribution is a proposed mixture of $[\mathbf{1}+\mathbf{2}+H]^+$, $[\mathbf{1}+\mathbf{2}-Cl+2H_2O]^+$, and $[\mathbf{1}+\mathbf{2}-C_{10}H_{14}+3\,CH_3OH+2\,H_2O+H]^+$ in the ratio of 2:5:1. The average deviation of the experimental relative abundances from the calculated values is shown in the upper right hand corner of (b). Each error bar represents one standard deviation calculated from three measurements, with ten spectra averaged per measurement.[20] Potential structures for the species formed when **3** or **4** reacts with **1** are in Figure S1 of the Supporting Information. Reactive species are not observed for **5**.

In the proposed mechanism for the bulk reaction the NH_2 and OH groups of **L** are in positions that allow simultaneous formation of stable bonds with the Ru atom (Scheme 1). Although the NH_2 group of **4** is not in the β position with respect to the OH functionality, rotation around the C–C bonds of the ethyl alcohol substituent produces a conformation that allows the formation of $\mathbf{4}^{\mathbf{II}}$, thereby facilitating the reaction. However, because **4** requires a specific structural orientation to react with **1**, the probability of forming $\mathbf{4}^{\mathbf{II}}$ is lower (i.e. the frequency factor of the Arrhenius equation is smaller) than the probability of forming $\mathbf{2}^{\mathbf{II}}$ and $\mathbf{3}^{\mathbf{II}}$. These results are in agreement with the observation that the $\mathbf{L}^{\mathbf{P}}$, intermediates (i.e., $\mathbf{L}^{\mathbf{I}}$, $\mathbf{L}^{\mathbf{II}}$, and $\mathbf{L}^{\mathbf{III}}$), and $\mathbf{L}^{\mathbf{C}}$ of **2** and **3** have higher abundances than the corresponding reactive species for **4**. When the NH_2 and OH groups are located at opposite ends of the molecule (**5**), the Ru atom cannot simultaneously form stable bonds with both functionalities, so no reactive species were observed regardless of the experimental conditions or concentration of the reactants.

Potential structures for the species at *m/z* 762 have Ru atoms with 18 valence electrons, if, in the latter two structures, one or both of the *p*-cymenes can adopt an η^2-coordination geometry (Figure 2a).[19] The average deviation[21] of the experimental relative abundances from the calculated values is 5 ± 1% (Figure 2b), thereby providing support for the proposed assignments. Similar structures for *m/z* 750 (see Figure S1 in the Supporting Information) have average isotopic deviations of 6 ± 1% from the calculated values (data not shown). The chemical structures for all the reactive species detected in Figure 1 could not be unambiguously determined (e.g., the structure of intermediate III could not be determined from the acquired mass spectra) because of the many isobaric species present in the mass spectra. However, the formation of these isotopic distributions depends on the relative positions of the NH_2 and OH groups (Scheme 1b), thus indicating that these species participate in the reaction.

The proposed structures for the reaction intermediates formed when **1** reacts with CH_3OH (*m/z* 634) are all stable 18 valence electron species (Scheme 2). These structures are produced by subsequent eliminations of H_2 from $[\mathbf{1}-3\,Cl+4\,CH_3OH-2H]^+$ (*m/z* 633) and $[\mathbf{1}-2\,Cl+3\,CH_3OH-H]^{+\cdot}$ (*m/z* 637), thus resulting in species that have formaldehyde coordinating with the Ru atom. The species at *m/z* 634 can be represented as $[m/z\ 633-xH_2]^+$ and $[m/z\ 637-yH_2]^+$, where *x* and *y* are the number of H_2 eliminations. The most abundant species formed from the reaction of **1** with CH_3OH is *m/z* 579, which is proposed to be a mixture of $[\mathbf{1}-Cl]^+$, $[\mathbf{1}-Cl+2H_2O-HCl]^+$, and $[\mathbf{1}-Cl-C_{10}H_{14}+3\,CH_3OH+2\,H_2O]^+$.

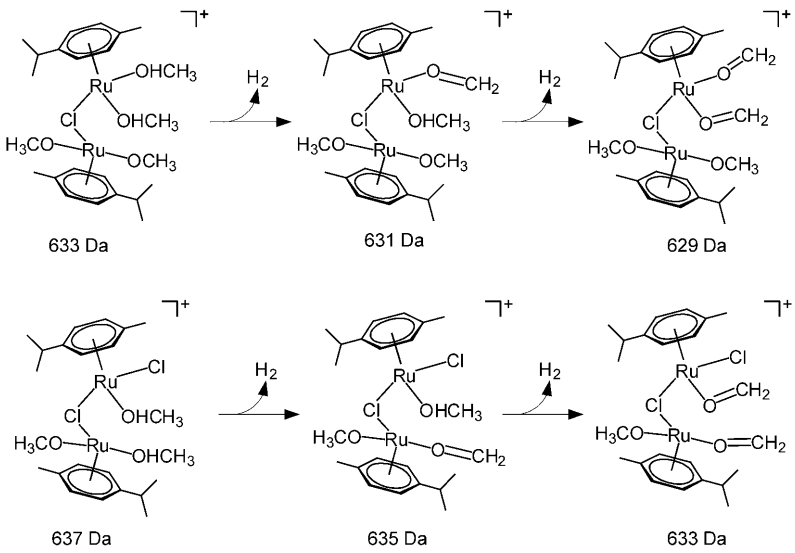

Scheme 2. Possible structures for some of the chemical species formed in the reaction of **1** with CH_3OH.

Finally, *m/z* 559 corresponds to $[\mathbf{1}-Cl+H_2O-HCl]^+$. For the three distributions, the average isotopic deviations are $5\pm1\%$ (calculated ratio of 2:2:5:3 for $x=0$, $x=2$, $y=0$, and $y=2$, respectively), $4\pm0\%$ (calculated ratio of 5:2:1), and $6\pm2\%$, respectively.

Dissociation of *m/z* 762 produces *m/z* 576 in tandem mass spectra (MS^n), which correspond to the loss of $[\mathbf{2}+H]^+$ and 36 Da (loss of $2H_2O$ or HCl). Further dissociation of *m/z* 576 (MS^3) produced three *m/z* distributions that are separated by approximately 36 Da (*m/z* 468, *m/z* 503, and *m/z* 540), which are caused by sequential loss of $2H_2O$ or HCl. This fragmentation pattern is confirmed by MS^4 experiments in which dissociation of *m/z* 540 produced fragments at *m/z* 503 and *m/z* 468, and dissociation of *m/z* 503 results in *m/z* 468. The fragment at *m/z* 468 is also observed in MS spectra for **4** and **5** but not for **2** and **3** (Figure 1), which suggests that reaction of **1** with β-amino alcohols is the preferred pathway. Fragments at *m/z* 289 and *m/z* 303 in the MS^2 spectra of *m/z* 762 involve the coordination of H_2O and CH_3OH with [RuCl(*p*-cymene)], respectively. The MS^3 spectra of *m/z* 634 (MS^2 of *m/z* 634 yields *m/z* 576) and the MS^2 spectra of *m/z* 579 for the reactions of **1** with **2** (or with **3**) and CH_3OH are similar, and this observation further supports the proposed structure of $\mathbf{2^{II}}$. In addition to these observations, dissociation of $\mathbf{2^{III}}$ and $\mathbf{2^{P}}$ both yield the signal at *m/z* 384, which supports the conclusion that these species are relevant to the reaction pathway. All of the trends and fragmentation patterns described above were also observed for **3**. The dissociation pathways observed in MS^n spectra agree with the proposed structures and mechanism, thus providing additional support for the proposed structures of the intermediates.

In addition to the proposed structures, other reactive species and fragments, as well as background ions were observed in DESI-MS spectra of the reactions of **L** with **1** (compare Figure 1b–e with Figure 1a). Background ion signals (e.g. *m/z* 487, *m/z* 513, and *m/z* 535 in Figure 1b) were distinguished from signals of reactive species by comparing the results in Figure 1b–1e to mass spectra acquired when **L** is sprayed on blank paper (data not shown). In these experiments, the isotope patterns of the ion signals are much simpler because they do not contain any Ru atoms, thus ruling them out as reactive species.

The concentration of the reactive species in the microdroplets can be estimated from the acquired ion currents. Using 0.0001% as a rough estimate of the transfer efficiency from the surface to the detector of the mass spectrometer,[22] approximately 10^{13}–10^{14} molecules of the identified reactive species of **2** are estimated to be formed when **2** (250 pmol impact the surface in 15 s) is reacted with approximately 10^{15} molecules[23] of **1** on the surface (ca. 15 μg deposited) for 15 seconds.[24] The diameter of the droplet leaving the surface is approximately 2 μm,[17] so the concentration of the reactive species in the droplets is estimated to be in the micromolar regime assuming that dry ions are not formed before entering the mass spectrometer.

DESI-MS allows chemical reactions that occur in microscale volumes (droplet volume of approximately 4 μm^3) to be probed in real time. As discussed above, the short timescales of desorption and ionization allow detection of reaction intermediates that have lifetimes on the order of milliseconds with high sensitivity (pmol quantities). These capabilities, coupled with the high-throughput features[3,5,6] and enhanced reaction rates in DESI microdroplets[25] should make it a powerful tool for elucidating reaction mechanisms. These discoveries open a new route for the study of novel chemistry through liquid-phase reactions.

Received: August 4, 2010
Revised: September 14, 2010
Published online: November 25, 2010

Keywords: mass spectrometry · organometallic catalysis · reaction intermediates · ruthenium · transfer hydrogenation

[1] a) J. C. Traeger, *Int. J. Mass Spectrom.* **2000**, *200*, 387–401; b) P. Chen, *Angew. Chem.* **2003**, *115*, 2938–2954; *Angew. Chem. Int. Ed.* **2003**, *42*, 2832–2847;; c) E. C. Meurer, L. S. Santos, R. A. Pilli, M. N. Eberlin, *Org. Lett.* **2003**, *5*, 1391–1394; d) A. A. Sabino, A. H. L. Machado, C. R. D. Correia, M. N. Eberlin, *Angew. Chem.* **2004**, *116*, 2568–2572; *Angew. Chem. Int. Ed.* **2004**, *43*, 2514–2518; e) D. Fabris, *Mass Spectrom. Rev.* **2005**, *24*, 30–54; f) M. N. Eberlin, *Eur. J. Mass Spectrom.* **2007**, *13*, 19–28; g) C. A. Marquez, H. Y. Wang, F. Fabbretti, J. O. Metzger, *J. Am. Chem. Soc.* **2008**, *130*, 17208–17209; h) L. S. Santos, *Eur. J. Org. Chem.* **2008**, 235–253; i) C. A. Muller, C. Markert, A. M. Teichert, A. Pfaltz, *Chem. Commun.* **2009**, 1607–1618; j) W. Schrader, P. P. Handayani, J. Zhou, B. List, *Angew. Chem.* **2009**, *121*, 1491–1494; *Angew. Chem. Int. Ed.* **2009**, *48*, 1463–1466.

[2] J. A. Kenny, K. Versluis, A. J. R. Heck, T. Walsgrove, M. Wills, *Chem. Commun.* **2000**, 99–100.

[3] a) Z. W. Takats, J. M. Wiseman, B. Gologan, R. G. Cooks, *Science* **2004**, *306*, 471 – 473; b) Z. Takats, J. M. Wiseman, R. G. Cooks, *J. Mass Spectrom.* **2005**, *40*, 1261 – 1275.

[4] a) A. Venter, M. Nefliu, R. G. Cooks, *Trac Trends Anal. Chem.* **2008**, *27*, 284 – 290; b) G. J. Van Berkel, S. P. Pasilis, O. Ovchinnikova, *J. Mass Spectrom.* **2008**, *43*, 1161 – 1180; c) X. X. Ma, M. X. Zhao, Z. Q. Lin, S. C. Zhang, C. D. Yang, X. R. Zhang, *Anal. Chem.* **2008**, *80*, 6131 – 6136; d) H. W. Chen, G. Gamez, R. Zenobi, *J. Am. Soc. Mass Spectrom.* **2009**, *20*, 1947 – 1963; e) G. K. Barbula, M. D. Robbins, O. K. Yoon, I. Zuleta, R. N. Zare, *Anal. Chem.* **2009**, *81*, 9035 – 9040; f) D. R. Ifa, C. P. Wu, Z. Ouyang, R. G. Cooks, *Analyst* **2010**, *135*, 669 – 681; g) D. J. Weston, *Analyst* **2010**, *135*, 661 – 668.

[5] R. G. Cooks, Z. Ouyang, Z. Takats, J. M. Wiseman, *Science* **2006**, *311*, 1566 – 1570.

[6] H. W. Chen, N. N. Talaty, Z. Takats, R. G. Cooks, *Anal. Chem.* **2005**, *77*, 6915 – 6927.

[7] a) A. B. Costa, R. G. Cooks, *Chem. Commun.* **2007**, 3915 – 3917; b) A. B. Costa, R. G. Cooks, *Chem. Phys. Lett.* **2008**, *464*, 1 – 8; c) A. Badu-Tawiah, C. Bland, D. I. Campbell, R. G. Cooks, *J. Am. Soc. Mass Spectrom.* **2010**, *21*, 572 – 579; d) L. Gao, G. T. Li, J. Cyriac, Z. X. Nie, R. G. Cooks, *J. Phys. Chem. C* **2010**, *114*, 5331 – 5337.

[8] a) I. Cotte-Rodriguez, Z. Takats, N. Talaty, H. W. Chen, R. G. Cooks, *Anal. Chem.* **2005**, *77*, 6755 – 6764; b) H. Chen, I. Cotte-Rodriguez, R. G. Cooks, *Chem. Commun.* **2006**, 597 – 599; c) L. Nyadong, M. D. Green, V. R. De Jesus, P. N. Newton, F. M. Fernandez, *Anal. Chem.* **2007**, *79*, 2150 – 2157; d) G. Huang, H. Chen, X. Zhang, R. G. Cooks, Z. Ouyang, *Anal. Chem.* **2007**, *79*, 8327 – 8332; e) Y. Song, R. G. Cooks, *J. Mass Spectrom.* **2007**, *42*, 1086 – 1092; f) L. Nyadong, E. G. Hohenstein, K. Johnson, C. D. Sherrill, M. D. Green, F. M. Fernandez, *Analyst* **2008**, *133*, 1513 – 1522; g) L. Nyadong, S. Late, M. D. Green, A. Banga, F. M. Fernandez, *J. Am. Soc. Mass Spectrom.* **2008**, *19*, 380 – 388; h) L. Nyadong, E. G. Hohenstein, A. Galhena, A. L. Lane, J. Kubanek, C. D. Sherrill, F. M. Fernandez, *Anal. Bioanal. Chem.* **2009**, *394*, 245 – 254; i) C. P. Wu, D. R. Ifa, N. E. Manicke, R. G. Cooks, *Anal. Chem.* **2009**, *81*, 7618 – 7624; j) Y. Zhang, H. Chen, *Int. J. Mass Spectrom.* **2010**, *289*, 98 – 107.

[9] M. J. Palmer, M. Wills, *Tetrahedron: Asymmetry* **1999**, *10*, 2045 – 2061.

[10] a) G. Zassinovich, G. Mestroni, S. Gladiali, *Chem. Rev.* **1992**, *92*, 1051 – 1069; b) S. Hashiguchi, A. Fujii, J. Takehara, T. Ikariya, R. Noyori, *J. Am. Chem. Soc.* **1995**, *117*, 7562 – 7563; c) A. Fujii, S. Hashiguchi, N. Uematsu, T. Ikariya, R. Noyori, *J. Am. Chem. Soc.* **1996**, *118*, 2521 – 2522; d) K. Matsumura, S. Hashiguchi, T. Ikariya, R. Noyori, *J. Am. Chem. Soc.* **1997**, *119*, 8738 – 8739.

[11] K. J. Haack, S. Hashiguchi, A. Fujii, T. Ikariya, R. Noyori, *Angew. Chem.* **1997**, *109*, 297 – 300; *Angew. Chem. Int. Ed. Engl.* **1997**, *36*, 285 – 288.

[12] a) J. B. Jones, *Tetrahedron* **1986**, *42*, 3351 – 3403; b) R. Noyori, S. Hashiguchi, *Acc. Chem. Res.* **1997**, *30*, 97 – 102.

[13] a) J. Takehara, S. Hashiguchi, A. Fujii, S. Inoue, T. Ikariya, R. Noyori, *Chem. Commun.* **1996**, 233 – 234; b) J. A. Kenny, M. J. Palmer, A. R. C. Smith, T. Walsgrove, M. Wills, *Synlett* **1999**, 1615 – 1617; c) K. Everaere, A. Mortreux, M. Bulliard, J. Brussee, A. van der Gen, G. Nowogrocki, J. F. Carpentier, *Eur. J. Org. Chem.* **2001**, 275 – 291; d) M. J. Palmer, J. A. Kenny, T. Walsgrove, A. M. Kawamoto, M. Wills, *J. Chem. Soc. Perkin Trans. 1* **2002**, 416 – 427.

[14] M. Palmer, T. Walsgrove, M. Wills, *J. Org. Chem.* **1997**, *62*, 5226 – 5228.

[15] The areas of the signals at *m/z* 372 and *m/z* 408 are obtained by integrating the *m/z* ranges 365.5–376.5 Da and 402.5–412.5 Da, respectively. The areas of the signals at *m/z* 384 and *m/z* 420 are obtained by integrating the *m/z* ranges 377.5–388.5 Da and 415.5–424.5 Da, respectively.

[16] The concentration of the solutions of **1** and **L** were 10^{-5} M in CH_2Cl_2 and 10^{-4} M in CH_3OH, respectively. Each reagent solution was infused into a static mixing tee (2 μL swept volume; Upchurch Scientific, Oak Harbor, WA, USA) at a flow rate of 5 $\mu L\,min^{-1}$. The N_2 flow rate was 0.6 $L\,min^{-1}$ and the spray voltage was 5 kV. The length of the fused silica tubing from the mixing tee to the tip of the ESI source is 50 cm and the internal diameter is 75 μm. The length of the inlet capillary of the mass spectrometer is 18.5 cm.

[17] A. Venter, P. E. Sojka, R. G. Cooks, *Anal. Chem.* **2006**, *78*, 8549 – 8555.

[18] The absolute abundances of each species are obtained by summing the intensities of all the ion signals in each distribution. The intensities of the ion signals in the *m/z* ranges 376–388 Da and 364–376 Da were summed for the reactions of **1** with **2** or with **3**, respectively. The intensities of the ion signals in the *m/z* range 550–800 Da were summed for each of the reactions of **1** with **4** or with **5** and CH_3OH.

[19] W. D. Harman, H. Taube, *J. Am. Chem. Soc.* **1988**, *110*, 7555 – 7557.

[20] Isotope ratios are calculated by using Qual Browser software from Thermo Fisher Scientific (San Jose, CA, USA) and only signals with a signal-to-noise greater than three were considered.

[21] The average deviation was determined by calculating the average value of | (theoretical relative abundance) − (calculated relative abundance) | for each isotope signal.

[22] The calculation of the transfer efficiency can be found in the Supporting Information.

[23] This is the actual amount of **1** on the surface that interacts with the droplets from the DESI source. Because the area of the spray at the surface ($0.1 \pm 0.0\ cm^2$) is smaller than the area of the sample spot ($0.8 \pm 0.2\ cm^2$), the amount of **1** actually sampled into the mass spectrometer per analysis is given by [(amount deposited/area of the sample spot) × (area of the spray at the surface)].

[24] a) R. D. Smith, J. A. Loo, C. G. Edmonds, C. J. Barinaga, H. R. Udseth, *Anal. Chem.* **1990**, *62*, 882 – 899; b) M. Busman, J. Sunner, C. R. Vogel, *J. Am. Soc. Mass Spectrom.* **1991**, *2*, 1 – 10; c) P. Kebarle, L. Tang, *Anal. Chem.* **1993**, *65*, A972 – A986; d) B. W. Lin, J. Sunner, *J. Am. Soc. Mass Spectrom.* **1994**, *5*, 873 – 885; e) D. R. Zook, A. P. Bruins, *Int. J. Mass Spectrom. Ion Processes* **1997**, *162*, 129 – 147; f) R. E. March, *J. Mass Spectrom.* **1997**, *32*, 351 – 369; g) N. B. Cech, C. G. Enke, *Mass Spectrom. Rev.* **2001**, *20*, 362 – 387; h) J. S. Page, R. T. Kelly, K. Tang, R. D. Smith, *J. Am. Soc. Mass Spectrom.* **2007**, *18*, 1582 – 1590.

[25] D. I. Campbell, M. Girod, E. Moyano, R. G. Cooks, unpublished results.

